Environ. Sci. Technol. **2010,** *44,* 2542–2548

Phenol Groups in Northeastern U.S. Submicrometer Aerosol Particles Produced from Seawater Sources

RANJIT BAHADUR,[†] TIMOTHY UPLINGER,[†] LYNN M. RUSSELL,*[,†] BARKLEY C. SIVE,[‡] STEVEN S. CLIFF,[¶] DYLAN B. MILLET,[§] ALLEN GOLDSTEIN,[||] AND TIMOTHY S. BATES[⊥]

Scripps Institution of Oceanography, University of California San Diego, La Jolla California 92093-0221, Institute for the Study of Earth, Ocean, and Space, University of New Hampshire, Durham New Hampshire 03824, Department of Applied Science, University of California, Davis, California 95616, Department of Soil, Water, and Climate, University of Minnesota, St. Paul, Minnesota 55108, Department of Environmental Science, Policy, and Management, University of California, Berkeley, California 94720, and Pacific Marine Environmental Laboratory, National Oceanic and Atmospheric Administration, Seattle, Washington 98115

Received October 25, 2009. Revised manuscript received January 29, 2010. Accepted February 11, 2010.

Atmospheric particles collected during the ICARTT 2004 field experiment at ground based sites at Appledore Island (AI), New Hampshire, Chebogue Point (CP), Nova Scotia, and aboard the R/V *Ronald Brown* (RB) were analyzed using Fourier transform infrared (FTIR) spectroscopy to quantify organic mass (OM) and organic functional groups. Several of these spectra contain a unique absorbance peak at 3500 cm^{-1}. Laboratory calibrations identify this peak with phenol functional groups. The phenol groups are associated with seawater-derived emissions based on correlations with tracer volatile organic compounds (VOCs) and ions, and potential source contribution function (PSCF) analysis. On the basis of the measured absorptivities, the project average phenol group concentrations are 0.24 ± 0.18 $\mu g\ m^{-3}$ (4% of the total OM) at AI, 0.10 ± 0.6 $\mu g\ m^{-3}$ (5% of the total OM) at CP, and 0.08 ± 0.09 $\mu g\ m^{-3}$ (2% of the total OM) on board the RB, with detection limits typically between 0.06 and 0.11 $\mu g\ m^{-3}$. The spectra were partitioned into three primary factors using positive matrix factorization (PMF) sufficient to explain more than 95% of the measured OM. The fossil fuel combustion factor contributed 40% (AI), 34% (CP), and 43% (RB) of the total OM; the terrestrial biogenic factor contributed 20% (AI), 30% (CP), and 27% (RB). The seawater-derived factor contributed 40% (AI), 36% (CP) and 29% (RB) of the OM and showed similar correlations to tracers as the phenol group.

* Corresponding author e-mail: lmrussell@ucsd.edu.
[†] Scripps Institution of Oceanography.
[‡] University of New Hampshire.
[¶] University of California, Davis.
[§] University of Minnesota.
[||] University of California, Berkeley.
[⊥] Pacific Marine Environmental Laboratory.

Introduction

The International Consortium for Atmospheric Research on Transport and Transformation field experiment (ICARTT 2004) was carried out during the summer of 2004 to study emissions, transport, and chemical transformations of gas and aerosol species in the Northeastern U.S. and their impact on air quality and climate on regional to intercontinental scales (*1*). As a part of this experiment, aerosol particles were collected in coastal New England—at ground sites at Chebogue Point (CP) and Appledore Island (AI) and aboard the R/V *Ronald Brown* (RB)—to quantify their organic fraction. In addition, the sampling platforms also included a suite of high time resolution measurements including gas and particle phase physical and chemical properties, as well as meteorological parameters (*1*−*6*). Pollution events at these sites were found to be highly episodic and were associated with specific emission sources based on analysis of coemitted tracers. At Chebogue Point, for example, distinct episodes associated with US pollution outflow (15% of measurement period), fresh and processed biogenic emissions, biomass burning, and local anthropogenic sources were identified (*7*). Onboard the R/V *Ronald Brown*, a factor analysis of the combined data on gas and aerosol species revealed that the aerosol organic mass measured during the study was predominantly of secondary anthropogenic origin (*3*). In addition to these continental sources, possible marine sources of organic aerosol were also identified (*8*). Back trajectory analysis indicated that forest fire plumes from Northern Canada and Alaska rarely mixed with the boundary layer and were a minor component of atmospheric measurements (*9*−*11*), suggesting that aerosols in this region are dominated by regional sources.

Infrared spectroscopy provides a well-developed methodology for quantitative measurements of functional groups in atmospheric aerosols that can be related to broad pollution sources (*12*−*15*). For example, long chain hydrocarbons (alkane and alkene groups) are usually characteristic of diesel and oil combustion (*16*), mixtures of carboxylic and nonacid carbonyl groups reflect secondary organic aerosol (SOA) (*17*), marine saccharides are a source of organic hydroxyl and amine mixtures (*18*), and nonacid carbonyl groups have been detected in biogenic emissions and the products of biomass burning (*19, 20*). The organic functional group compositions of many sources include overlapping characteristics and cannot be used as specific molecular tracers for the purposes of source apportionment. In previous work, we presented the analysis of major functional groups in aerosol samples measured during the ICARTT experiment (*15*). Example absorption spectra and corresponding functional group compositions are illustrated in Figure 1a. A total of 197 ICARTT spectra (out of 322) contain a unique and sharp absorption peak at 3500 cm^{-1} above the broad organic hydroxyl absorption that has not been observed at other urban or remote sites in prior FTIR sampling (*13*−*15, 21*−*24*). In the present work we identify phenol as the functional group having this absorption feature and identify its sources during ICARTT 2004.

Experimental Section

Submicrometer particles were collected on 37 mm Teflon filters at AI (108 samples), CP (115 samples), and the RB (99 samples) over time periods between 6 and 24 h. Simultaneous field blanks were also collected for each sample. Details of the FTIR sampling sites and filter handling are summarized in the Supporting Information and described by Gilardoni

10.1021/es9032277

Published on Web 03/01/2010

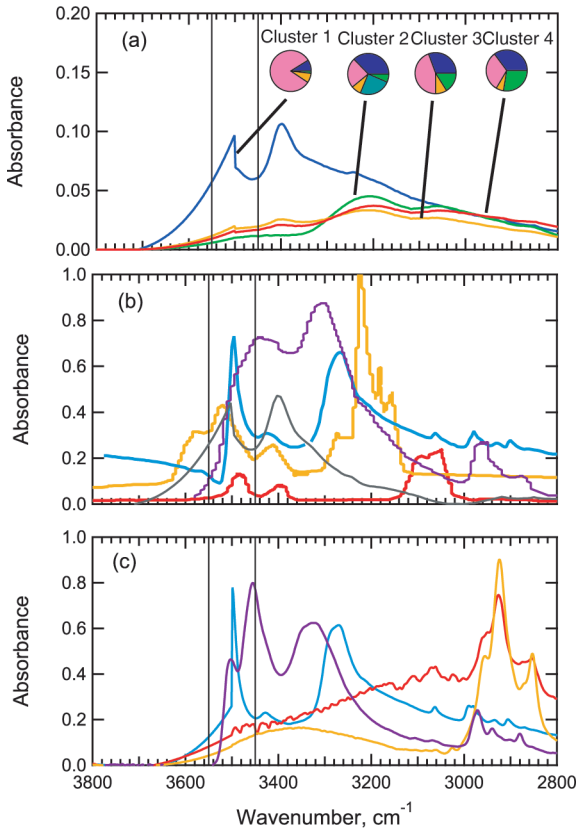

FIGURE 1. ICARTT spectra clusters, database standards, and laboratory standard spectra showing phenol absorption at 3500 cm^{-1}. (a) Representative spectra from ward clusters 1 (blue), 2 (green), 3 (orange), and 4 (red) shown along with their corresponding functional group composition as alkanes (blue), hydroxyl (pink), carbonyl (teal), amines (orange), and acid (green) illustrated in pie charts 1−4. (b) Reference spectra for 1,2-benzene diamine (red), 4-tert-butyl benzene amine (orange), ethyl 3,4-dihydroxy benzoate (purple), *n*-propyl 3,4,5-trihydroxy benzoate (blue), and lignin (gray). (c) Spectra for aerosolized standards deposited and dried on Teflon filters in the same colors as panel b.

and co-workers (*15*). FTIR absorbance of a detected organic species varies linearly with its mass loading and is independent of the mixture composition (*13, 14*). The bulk of organic mass in ambient aerosol samples comprises alkane (quantified between 2790−2930 cm^{-1}), carboxylic acid and nonacid carbonyl (1720 cm^{-1}), organic hydroxyl (3100−3400 cm^{-1}), and primary amine (1630 cm^{-1}) groups, with alkene (2980 cm^{-1}), aromatic (3050 cm^{-1}), and organosulfate groups (876 cm^{-1}, by rinsing) typically below the detection limit for ICARTT (*15*). Since FTIR absorption varies linearly with mass loading of organic functional groups, similarities in absorption spectra reflect similarities in the relative amounts of functional groups in ambient samples that in turn reflect similarities in possible primary and secondary sources (*25*). The Ward algorithm (*26*) was used to hierarchically cluster absorption spectra normalized with respect to the absorbance maxima into four main clusters that contain different relative amounts of alkane, organic hydroxyl, carbonyl, and acid groups. Increasing the number of branches subdivided these clusters into smaller groups with minor differences in relative composition. The striking feature of the average spectra illustrated in Figure 1a is that adjacent to the broad organic hydroxyl group absorption between 3100 and 3400 cm^{-1} is a narrow absorption peak at 3500 cm^{-1}, which has not been identified previously in atmospheric aerosol samples.

Narrow Absorption at 3500 cm^{-1}. To identify the source of absorption at 3500 cm^{-1}, IR spectra for organic compounds

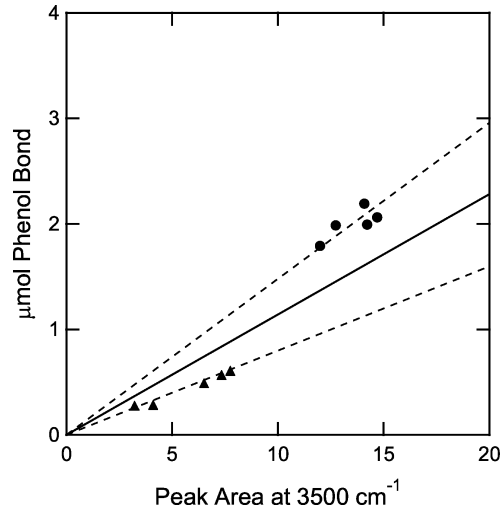

FIGURE 2. Calibration lines for IR absorption by phenols at 3500 cm^{-1}. Triangles are *n*-propyl 3,4,5-trihydroxy benzoate samples, and circles are ethyl 3,4-dihydroxy benzoate samples. Dashed lines show regression lines for individual standards and the solid line shows the average calibration assuming an equimolar mixture.

maintained in standard reference libraries (*27, 28*) were examined to locate significant peaks around 3500 ± 20 cm^{-1}. This criterion is satisfied by aromatic amines (for example, 1,2-benzene diamine and 4-tert-butyl benzene amine) and polyfunctional phenols (for example, ethyl 3,4-dihydroxy benzoate and *n*-propyl 3,4,5-trihydroxy benzoate). The standard absorption spectra for these compounds are illustrated in Figure 1b. Calibration standards for the selected compounds were prepared, handled, and analyzed as described in the Supporting Information.

FTIR spectra for the prepared laboratory standards of ethyl 3,4-dihydroxy benzoate and *n*-propyl 3,4,5-trihydroxybenzoate, illustrated in Figure 1c, contain a narrow absorption peak at 3500 cm^{-1} that is very similar to the structure observed in ambient samples. In contrast, 1,2-benzene diamine and 4-tert-butyl benzene amine do not absorb sufficiently to produce an absorption signal above the noise in the spectra despite this structure's presence in NIST database spectra. This difference can be explained by the detector sensitivities of the spectrometers in the 3000−3600 cm^{-1} range, matrix effects, and differences in sample preparation. The NIST standards were scanned in the solid phase using the DOW-KBr foresprism grating instrument, with a range of operation between 1300 and 3800 cm^{-1}, and details on the detector used were not specified. The Bruker Tensor 27 model used in this work has an operational range from 400 to 4000 cm^{-1}, with the DTGS detector having high sensitivity in the 2500−3500 cm^{-1} region. We conclude that the peak at 3500 cm^{-1} in the ambient spectra is due to absorption by phenol moieties. The reference spectrum of wood samples (containing multiple organic hydroxyl and phenolic groups from lignin structures) shows strong absorption between 3200 and 3500 cm^{-1} with a narrow peak at 3500 cm^{-1} (*29, 30*), consistent with the identification of the phenol group with the absorption at 3500 cm^{-1}. The absorbance of the calibration standards varied linearly with the number of moles of bonds and mass loading independent of mixture composition and is shown in Figure 2. A standardized major axis (SMA) regression between absorbance and loading for the two standards yields a slope of 0.092 μmol-bond area^{-1} for *n*-propyl 3,4,5-trihydroxybenzoate (with correlation coefficient, $R = 0.97$) and 0.154 μmol-bond area^{-1} for ethyl 3,4-dihydroxy benzoate ($R = 0.77$). These two standards provide a good first approximation of phenol group absorptivity in atmospheric

particles, and as such, we base the absorptivity for ambient samples on their arithmetic mean. The inverse absorptivity is then 0.123 μmol-bond area^{-1} at 3500 cm^{-1}, compared to 0.057 μmol-bond area^{-1} for the broader peak associated with linear chain organic hydroxyls and other polyols (*23*). The difference in absorptivities of the two laboratory standards results in an uncertainty of 25% in phenol mass, in addition to an uncertainty between 5−22% introduced by interference from water, ammonium, and primary amines between 3300 and 3600 cm^{-1} (*14*). Once specific molecular standards for phenol groups present in atmospheric particles can be identified, a more accurate absorptivity can be calculated. However, the impact on total organic mass (OM) would be negligible due to the relatively small phenol group mass fraction. The lower inverse absorptivity (fewer bonds per unit absorption area) at 3500 cm^{-1} for the phenol group than at 3050 cm^{-1} for the aromatic group (8.7 μmol-bond area^{-1}) makes the latter group more difficult to resolve in the ICARTT samples even though it co-occurs with the phenol groups.

Analysis of Ambient ICARTT Spectra. Positive matrix factorization (PMF) was applied to baselined FTIR spectra to decompose the complex ambient samples into a smaller number of primary components (*22, 23, 31*), with computational details in the Supporting Information. Sources associated with each factor were identified using SMA regression with comeasured volatile organice compounds (VOCs) from PTR-MS and GCMS measurements (*2−5, 7, 9, 11, 32−36*), X-ray fluorescence (XRF) metals (CP) (*37*), and ions from Particle into liquid sampler (PILS) and impactor measurements (RB) (*3*). Hierarchical Ward clustering was used to segregate all ambient samples into a smaller number of clusters, each of which was dominated by a different combination of source factors. The potential source contribution function (PSCF) (*38*) was used to determine the most probable geographic source regions for each source factor based on HYSPLIT (*39*) air mass back-trajectories.

Results

Quantification of Phenol Groups in ICARTT. The concentrations of phenol and nonphenol hydroxyl groups are compared in Figure 3a, grouped by Ward cluster. The narrow phenol group absorption peak at 3500 cm^{-1} could not be decoupled from the broad organic hydroxyl group (3100−3400 cm^{-1}) background in 39% of the total spectra quantified and was determined to be below the detection limit, which increases with the hydroxyl to phenol ratio and varies between 0.06 and 0.11 μg m^{-3} for ICARTT. A majority of filter samples at AI (66%) and CP (64%) contained phenol concentrations above the detection limit, compared to only 32% of the samples from the RB. Phenol group concentrations below the detection limit are set to 0 (a lower bound). Organic hydroxyl groups compose 70% of the OM in cluster 1 (31 total spectra) with the remainder comprised of alkane and primary amine groups. Spectra in this cluster contain the largest phenol absorption peaks, which yield the largest absolute concentration (mean and standard deviation of 0.56 ± 0.15 μg m^{-3}) and contribution to total organic hydroxyl group mass (15−23%) from phenol groups. Cluster 2 (48 spectra) is characterized by a large carbonyl fraction, which contributes 34% of the mass, a correspondingly smaller fraction of organic hydroxyl groups (19%), and the smallest relative phenol group absorption. The average phenol group concentration is 0.13 ± 0.05 μg m^{-3}, composing 13% of the organic hydroxyl group mass. Clusters 3 (46 spectra) and 4 (58 spectra) consist of 35% alkane groups with different ratios of carboxylic acids and hydroxyl groups constituting the remaining OM. The average phenol group concentration for clusters 3 and 4 is 0.19 ± 0.04 μg m^{-3} (14−16% of organic hydroxyl group mass) and 0.14 ± 0.04 μg m^{-3} (11−14% of organic hydroxyl group mass), respectively. The correlation

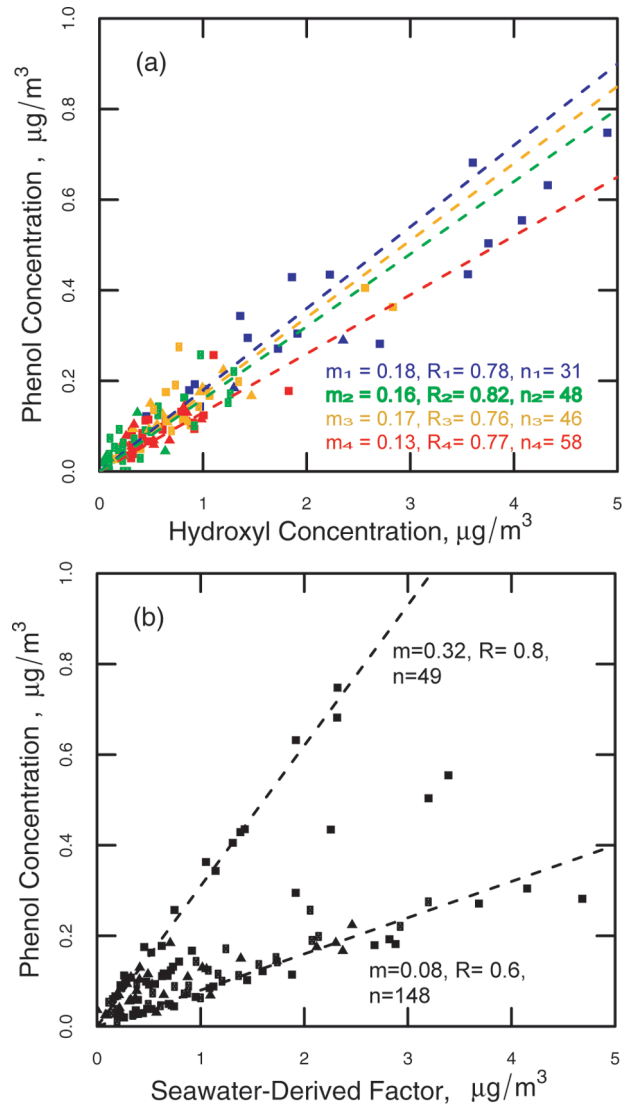

FIGURE 3. (a) Comparison between phenol and nonphenol hydroxyl concentrations for ambient ICARTT samples. Squares are from AI, triangles, from CP, and circles, from the RB. The markers are colored according to the hierarchical clusters illustrated in Figure 1. SMA regression lines with slope (*m*), correlation (*R*), and number (*n*) are illustrated. (b) Comparison of phenol group concentration with PMF seawater-derived factor. The higher line corresponds to transport from the Gulf of Maine, and the lower line corresponds to transport from the Atlantic or over land.

between phenol and nonphenol hydroxyl group concentrations is very strong ($R > 0.75$) for each of the clusters suggesting that both functional groups have the same sources.

The project mean and standard deviation for the phenol group concentration at AI is 0.24 ± 0.18 μg m^{-3} (or 0.33 ± 0.12 μg m^{-3} for only ADL samples, composing 5−11% of the OM for these samples). The phenol group concentration shows a weak correlation ($0.25 < R < 0.50$) with methyl chloride, methyl bromide, and carbonyl sulfide. Local wind directions vary between 0 and 90 deg (North East, corresponding to the direction of the Gulf of Maine) for periods with phenol group concentration above the 75th percentile (greater than 0.4 μg m^{-3}). Average wind speeds during these times were elevated at 5.8 m s^{-1} compared to the project average of 5.6 m s^{-1}. The CP phenol group concentration is 0.10 ± 0.06 μg m^{-3} (or 0.16 ± 0.04 μg m^{-3} for only ADL, constituting 5−9% OM). Weak correlations ($0.25 < R < 0.5$) exist for phenol group concentrations only with formaldehyde

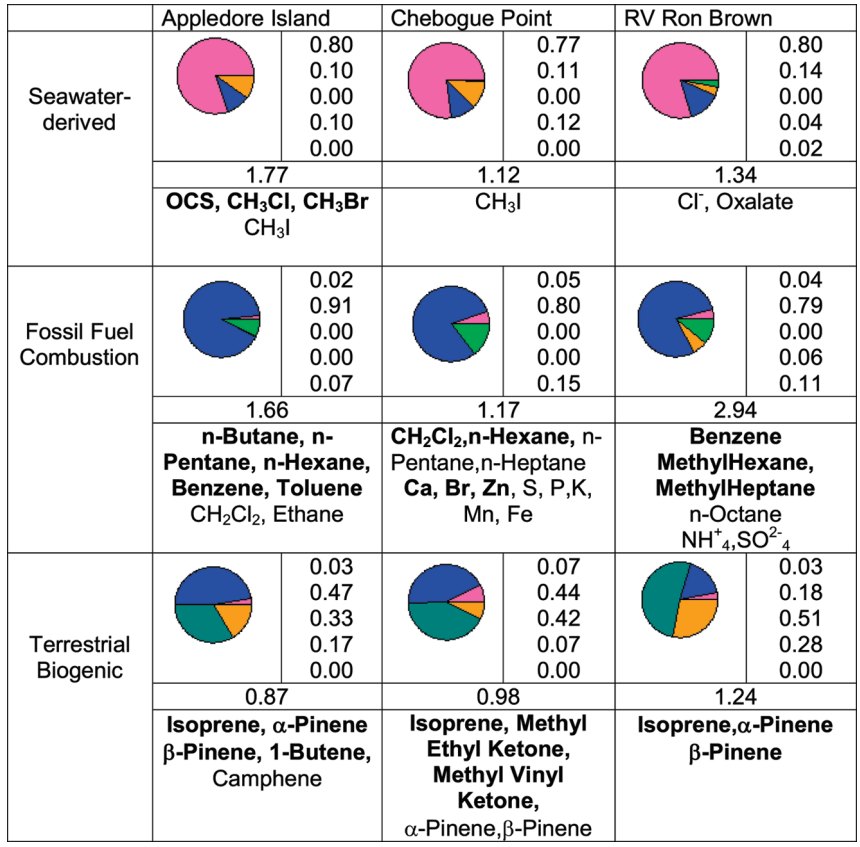

FIGURE 4. Compositions of the PMF factors, time-averaged project concentrations, and primarily correlated tracers by sampling platform. Relative contribution from the above detection limit functional groups in the pie charts is from organic hydroxyl (pink), alkane (blue), noncarboxylic carbonyl (teal), amine (orange), and carboxylic acid (green), and they are listed top to bottom, respectively. The average project concentration for each factor is in micrograms per cubic meter. Elemental and VOC tracers correlated with $R > 0.5$ (bold) and $0.5 > R > 0.25$ are listed.

and pentanone concentrations. The local wind direction for phenol group concentrations above the 75th percentile is between 150 and 210 deg (South−South West, corresponding to the directions of the Gulf of Maine and North American mainland) with average wind speeds of 3.3 m s^{-1} (3.1 m s^{-1} project average). The phenol group concentration for the RB is 0.08 ± 0.09 μg m^{-3} (or 0.15 ± 0.06 μg m^{-3} for only ADL, composing 2−6% OM), with no correlations of $R > 0.25$ with any of the measured tracer compounds. Phenol group concentrations above the 75th percentile (higher than 0.10 μg m^{-3}) correspond to average wind speeds of 5.5 m s^{-1} (4.9 m s^{-1} for the entire project). The ship was located in an area between 42N and 44N, and 69W and 71W during these periods with local winds from directions between 30 and 130 deg (East) again corresponding to the Gulf of Maine.

PMF of ICARTT FTIR Spectra. ICARTT aerosol samples were typically collected for 6−24 h and contain contributions from multiple sources. PMF analysis provides a technique for deconvoluting mixed samples by extracting correlated variables corresponding to similarities in sources, transport, and chemistry (*4, 7, 22, 23, 40*). For the three measuring platforms, solutions utilizing between three and six factors were found to reproduce 90−110% of the measured organic mass for each sample and to produce factors with smooth spectral shapes similar to known organic standards. A two factor solution reproduced less than 80% of the measured OM, and the use of more than seven factors resulted in factors with a low signal-to-noise ratio and a large overestimation in OM (as much as 30%) due to poor representation of the carboxylic COH and ammonium absorption peaks. Three unique types of factors persisted in all solutions that represented 90−110% of the measured OM, and these findings were identified as fossil-fuel combustion, terrestrial biogenic, and seawater-derived. The three-factor solution shows excellent agreement with measurements, reproducing 98% (AI), 110% (CP), and 99% (RB) of the average OM, with correlation coefficients between 0.90 and 0.92 in each case, indicating that this solution reproduces the structure of the measured spectra without introducing systematic errors. Project average functional group compositions, contributions to OM, and strong tracer correlations for the three factor solution are illustrated in Figure 4.

Discussion

Gas phase phenols and methyl halides in the atmosphere have been attributed to products of lignin (wood) burning (*41*−*43*), indicating that forest fires (or local biomass burning) are possible sources of the phenol groups measured in the atmosphere. The similarity between the absorption peak at 3500 cm^{-1} in the spectrum for lignin pulp and ICARTT cluster 1 spectra (Figure 1) further suggests that the phenolic groups are derived from plant material or its combustion. However, typical atmospheric biomass burning tracers such as acetonitrile, acetone, and non sea-salt potassium (*7, 22*) show no correlation ($R < 0.25$ in all cases) to the phenol group concentrations measured during ICARTT. In addition to being wood burning tracers, methyl halides also have marine sources (*44*), as does formaldehyde (*45*). Local meteorology at each of the three platforms (elevated wind speeds and direction) indicates that air masses containing phenol groups originated over the Gulf of Maine rather than the North American land mass. On the basis of these observations, we propose that phenol groups during ICARTT were most likely resuspended as sea-spray to the atmosphere (*18, 46*). While it is beyond the scope of these aerosol measurements to

identify the source of phenol groups to seawater in the Gulf of Maine, other studies have attributed dissolved phenol groups measured in seawater samples (*47*) to a combination of riverine input (*48*), sediment resuspension, deposition of biomass burning products (*49*), and production from coastal macro-algae (*50, 51*). These mechanisms result in higher concentrations in near-coastal and surface waters, consistent with the higher amounts of phenol groups observed at the coastal sites (AI and CP).

PMF-Based Source Factors. Figure 4 illustrates the functional group composition of the three factors identified at each platform. The factors show consistent compositions in each case, with comparable functional group contributions. SMA regressions between factor concentration and VOC tracers (*7, 36*) with $R > 0.25$ are used to associate each factor with its most probable source. The first factor is identified as seawater-derived based on its correlation to oceanic tracers such as methyl halides (*52, 53*) and carbonyl sulfide (*54*) (with $0.5 > R > 0.25$) and the location of its potential source regions. The RB factor correlates to chloride and oxalate ion concentrations ($0.5 > R > 0.25$) and no VOCs. Organic hydroxyl groups dominate the seawater-derived factor and compose between 70% and 80% of the OM. Alkane and primary amine groups compose approximately equal fractions of the remaining OM, between 10% and 15% with minor contributions from carbonyl containing groups. Phenol groups compose 42% (AI), 35% (CP), and 19% (RB) of the total organic hydroxyl group mass in the seawater-derived factor. OM has been shown to be transferred from the organic matter components in the ocean to atmospheric particles by wave-induced bubble bursting (*18, 55*). This mechanism also provides a way to transfer phenol groups found in surface seawater to atmospheric particles. The project mean concentration and standard deviation for this factor is 1.77 ± 0.31 $\mu g\ m^{-3}$ at AI (between 14% and 73% for individual samples), 1.12 ± 0.18 $\mu g\ m^{-3}$ at CP (between 11% and 58%), and 1.34 ± 0.24 $\mu g\ m^{-3}$ aboard the RB (between 3% and 45%). Phenol group concentrations show two very distinct relationships (Figure 3) to the seawater-derived factor, with slopes of 0.30 ± 0.06 and 0.08 ± 0.03 and $R > 0.7$ in both cases. The higher slope corresponds to samples from air masses from the Gulf of Maine (high phenol group concentration) while the lower slope corresponds to samples from air masses from over land or the Atlantic Ocean, consistent with higher phenol concentrations in the coastal waters of the Gulf of Maine.

The second factor is attributed to fossil fuel combustion. The project average concentration for this factor is 1.66 ± 0.32 $\mu g\ m^{-3}$ at AI (between 12% and 69% for individual samples), 1.17 ± 0.18 $\mu g\ m^{-3}$ at CP (between 4% and 81%), and 2.94 ± 0.81 $\mu g\ m^{-3}$ aboard the RB (between 26% and 92%). The combustion factor is dominated by saturated alkane groups (contributing between 80 and 90% of the total mass) typically produced by the use of petroleum products (*7, 16*). Carboxylic acid groups compose 10% of the mass and are associated with SOA formed by the oxidation of combustion products. The factor has mild to strong correlations ($R > 0.5$) with tracers of combustion and urban pollution such as long and branched chain alkanes, benzene, toluene, and dichlomethane in the gas phase (*7, 16*). At CP, the combustion factor correlates to midly to Br ($R > 0.5$), crustal elements Ca and Zn ($R > 0.5$), and weakly to S and P ($0.5 > R > 0.25$), indicating a possible secondary contribution (*22*).

The third factor is attributed to SOA formation from terrestrial biogenic emissions. The average concentration is 0.87 ± 0.12 $\mu g\ m^{-3}$ at AI (between 2% and 45% for individual samples), 0.98 ± 0.14 $\mu g\ m^{-3}$ at CP (between 9% and 53%), and 1.24 ± 0.22 $\mu g\ m^{-3}$ aboard the RB (between 1% and 41%). This factor is characterized by large fractions of nonacid carbonyl and primary amine groups and correlates strongly to biogenic terpenoid compounds (isoprene, α-pinene, β-pinene, and camphene), as well as to oxygenated VOCs such as methyl-ethyl ketone (MEK) and methyl-vinyl ketone (MVK) that have biogenic sources (*7, 56*). A lack of correlation with combustion tracers such as K, acetone, and acetonitrile support the identification of this factor as secondary biogenic particles rather than biomass burning emissions. Phenol groups do not contribute significant mass to either the combustion or biogenic factors.

Source Regions. PSCF analysis of air mass back trajectories for each factor identified at the ICARTT sites provides a consistency check on the locations of identified sources, with details provided in the Supporting Information. The probable source regions for the phenol-containing factor are located in North American coastal waters and disperse areas of the Atlantic Ocean, consistent with the attribution of this source to ocean-derived particles. The combustion factors have high-probability source regions over New England, Nova Scotia, and shipping lanes in the Atlantic Ocean; however, the large urban areas on the East coast are not strongly indicated. This is consistent with the episodic nature of Northeastern U.S. pollution, as back-trajectories associated with both high and low aerosol concentrations tend to traverse the same locations. High probability source regions for the terrestrial biogenic factor are located in New England and the United States−Canada border, but these regions cannot be distinguished from the combustion source regions within the uncertainty of the method. The two continental factors associated with biogenic and combustion sources tend to covary in time, which is not surprising since their sources are located in similar regions. A factor based analysis of VOCs at CP suggested source regions consistent with our results (*7*).

We conclude that phenol groups in seawater derived from riverine input, sediment suspension, airborne deposition, and algal production contribute as much as 0.6 $\mu g\ m^{-3}$ (10% of total OM) to ambient aerosols for some periods and regions of the ICARTT 2004 experiment. A factor based analysis of ambient spectra is consistent with this result as the phenol group constitutes between 19 and 42% of the seawater-derived factor and a negligible fraction of the fossil fuel combustion and terrestrial biogenic factors. The strong phenol group signature present in ICARTT samples is unique to the Northeastern U.S. region, based on ambient sampling by FTIR to date (*13−15, 21−24*). The apparently unique feature of coastal waters in this region is consistent with past measurements of seawater composition. The location and persistence of the phenol feature is supported by the detection of an absorption signal at 3500 cm^{-1} during the ICEALOT 2008 cruise aboard the R/V *Knorr*, in three samples collected between March 23 and 26 as the ship crossed the St. Lawrence seaway south of Newfoundland (*23*).

Acknowledgments

The analysis of ICARTT measurements presented here was supported by a grant from BP. The opinions, findings, conclusions, and recommendations are those of the authors and do not necessarily reflect the views of BP. The ICARTT measurements used in this work were collected as part of projects supported by NOAA (including NA17RJ1231), NSF (including ATM04-01611), and the James S. McDonnell Foundation. Joost deGouw, Bill Kuster, Paul Goldan, Rupert Holzinger, and Patricia Quinn provided measurements used in this work.

Supporting Information Available

Computational details of PMF and PSCF analysis, absoprtion spectra of three primary PMF based factors and their respective time series, and details on source regions for the

seawater-derived factor from PSCF analysis. This material is available free of charge via the Internet at http://pubs.acs.org.

Literature Cited

(1) Fehsenfeld, F. C. International Consortium for Atmospheric Research on Transport and Transformation (ICARTT): North America to Europe - Overview of the 2004 summer field study. *J. Geophys. Res.−Atmos.* **2006**, *111*, D23S01.

(2) Fischer, E.; Pszenny, A. A. P.; Keene, W.; Maben, J.; Smith, A.; Stohl, A.; Talbot, R. Nitric acid phase partitioning and cycling in the New England coastal tmosphere. *J. Geophys. Res.* **2006**, *111*, D23S09.

(3) Quinn, P. K.; Bates, T. S.; Coffman, D.; Onasch, T. B.; Worsnop, D.; Baynard, T.; de Gouw, J. A.; Goldan, P. D.; Kuster, W. C.; Williams, E.; Roberts, J. M.; Lerner, B.; Stohl, A.; Pettersson, A.; Lovejoy, E. R. Impacts of sources and aging on submicrometer aerosol properties in the marine boundary layer across the Gulf of Maine. *J. Geophys. Res.−Atmos.* **2006**, *111*, D23.

(4) Williams, B. J.; Goldstein, A. H.; Millet, D. B.; Holzinger, R.; Kreisberg, N. M.; Hering, S. V.; White, A. B.; Worsnop, D. R.; Allan, J. D.; Jimenez, J. L. Chemical speciation of organic aerosol during the International Consortium for Atmospheric Research on Transport and Transformation 2004: Results from in situ measurements. *J. Geophys. Res.* **2007**, *112*, D10S26.

(5) Russell, L. M.; Mensah, A. A.; Fishcher, E. V.; Sive, B. C. S.; Varner, R. K. V.; Keene, W. C.; Stutz, J.; Pszenny, A. A. P. P. Nanoparticle growth following photochemical α- and β-inene oxidation at Appledore Island during International Consortium for Research on Transport and Transformation/Chemistry of Halogens at the Isles of Shoals 2004. *J. Geophys. Res.* **2007**, *112*, D10S21.

(6) International Consortium for Atmospheric Research on Transport and Transformation Data Management. 2004, http://esrl.noaa.gov/csd/ICARTT/studycoordination/wgdm.shtml. Accessed on 01/2010.

(7) Millet, D. B.; Goldstein, A. H.; Holzinger, R.; Williams, B. J.; Allan, J. D.; Jimenez, J. L.; Worsnop, D. R.; M., R. J.; White, A. B.; Hudman, R. C.; Bertschi, I. T.; Stohl, A. Chemical characteristics of North American surface layer outflow: Insights from Chebogue Point, Nova Scotia. *J. Geophys. Res.* **2006**, *111*, D23S53.

(8) Williams, B. J.; Goldstein, A. H.; Kreisberg, N. M.; Hering, S. V. An in-situ instrument for speciated organic composition of atmospheric aerosols: Thermal desorption aerosol GC/MSFID (TAG). *Aerosol Sci. Technol.* **2006**, *40*, 620–638.

(9) Warneke, C.; et al. Biomass burning and anthropogenic sources of CO over New England in the summer 2004. *J. Geophys. Res.−Atmos.* **2006**, *111*, D23S15.

(10) Duck, T.; Firanski, B.; Millet, D.; Goldstein, A.; Allan, J.; Holzinger, R.; Worsnop, D.; White, A.; Stohl, A.; Dickinson, C.; van Donkelaar, A. Transport of forest fire emissions from Alaska and the Yukon Territory to Nova Scotia during Summer 2004. *J. Geophys. Res.* **2007**, *112*, D10S44.

(11) de Gouw, J. A.; et al. Sources of particulate matter in the northeastern United States in summer: 1. Direct emissions and secondary formation of organic matter in urban plumes. *J. Geophys. Res.* **2008**, *111*, D08301.

(12) Blanco, A. J.; McIntyre, R. G. Infrared spectroscopic view of atmospheric particulates over El Paso, Texas. *Atmos. Environ.* **1972**, *6*, 557–562.

(13) Maria, S. F.; Russell, L. M.; Turpin, B. J.; Porcja, R. J. FTIR measurements of functional groups and organic mass in aerosol samples over the Caribbean. *Atmos. Environ.* **2002**, *36*, 5185–5196.

(14) Maria, S. F.; Russell, L. M.; Turpin, B. J.; Porcja, R. J.; Campos, T. L.; Weber, R. J.; Huebert, B. J. Source signatures of carbon monoxide and organic functional groups in Asian Pacific Regional Aerosol Characterization Experiment (ACE-Asia) submicron aerosol types. *J. Geophys. Res.−Atmos.* **2003**, *108*, 8637−8650.

(15) Gilardoni, S.; Russell, L. M.; Sorooshian, A.; Flagan, R. C.; Seinfeld, J. H.; Bates, T. S.; Quinn, P. K.; Allan, J. D.; Williams, B.; Goldstein, A. H.; Onasch, T. B.; Worsnop, D. R. Regional variation of organic functional groups in aerosol particles on four U.S. east coast platforms during the International Consortium for Atmospheric Research on Transport and Transformation 2004 campaign. *J. Geophys. Res.* **2007**, *112*, D10S27.

(16) Rogge, W. F.; Mazurek, M. A.; Hildemann, L. M.; Cass, G. R.; Simoneit, B. R. T. Quantification of Urban Organic Aerosols at a Molecular-Level - Identification, Abundance and Seasonal-Variation. *Atmos. Environ. Part A−Gen. Top.* **1993**, *27*, 1309–1330.

(17) Lim, Y. B.; Ziemann, P. J. Products and mechanism of secondary organic aerosol formation from reaction of n-alkanes with OH radicals in the presence of NOx. *Environ. Sci. Technol.* **2005**, *39*, 9229–9236.

(18) Russell, L. M.; Hawkins, L. N.; Frossard, A. A.; Quinn, P. K.; Bates, T. S. Carbohydrate-Like Composition of Submicron Atmospheric Particles and their Production from Ocean Bubble Bursting. *Proc. Natl. Acad. Sci.*, published online Dec 23, 2009; http://dx.doi.org/10.1073/PNAS.0908905107.

(19) Simoneit, B. R. T.; Mazurek, M. A. Organic matter of the troposphere. II. Natural background of biogenic lipid matter in aerosols over the rural western United States. *Atmos. Environ.* **1982**, *16*, 1967–1989.

(20) Graham, B.; Guyon, P.; Taylor, P. E.; Artaxo, P.; Maenhaut, W.; Glovsky, M. M.; Flagan, R. C.; Andreae, M. O. Organic compounds present in the natural Amazonian aerosol: Characterization by gas chromatography-mass spectrometry. *J. Geophys. Res.−Atmos.* **2003**, *108*, D244766.

(21) Maria, S. F.; Russell, L. M. Organic and Inorganic Aerosol Below-Cloud Scavenging by Suburban New Jersey Precipitation. *Atmos. Environ.* **2005**, *39*, 4793–4800.

(22) Liu, S.; Takahama, S.; Russell, L. M.; Gilardoni, S.; Baumgardner, D. Oxygenated organic functional groups and their sources in single and submicron organic particles in MILAGRO 2006 campaign. *Atmos. Chem. Phys. Discuss.* **2009**, *9*, 4567–4607.

(23) Russell, L. M.; Takahama, S.; Liu, S.; Hawkins, L. N.; Covert, D. S.; Quinn, P. K.; Bates, T. S. Oxygenated Fraction and Mass of Organic Aerosol from Direct Emission and Atmospheric Processing Measured on the R/V Ronald Brown during TEXAQS/GoMACCS 2006. *J. Geophys. Res.−Atmos.* **2009**, *114*, D00F05.

(24) Day, D. A.; Takahama, S.; Gilardoni, S.; Russell, L. M. Organic composition of single and submicron particles in different regions of western North America and the eastern Pacific during INTEX-B 2006. *Atmos. Chem. Phys. Discuss.* **2009**, *9*, 6657–6690.

(25) Russell, L. M.; Bahadur, R.; Hawkins, L. N.; Allen, J. A.; Baumgardner, D.; Quinn, P. K.; Bates, T. S. Organic Aerosol Characterization by Complementary Measurements of Chemical Bonds and Molecular Fragments. *Atmos. Environ.* **2009**, *43*, 6100–6105.

(26) Ward, J. Hierarchical grouping to optimize an objective function. *J. Am. Stat. Assoc.* **1963**, *58*, 236–244.

(27) National Institute of Advanced Industrial Science and Technology. http://riodb01.ibase.aist.go.jp/sdbs/. Accessed on 10/2009.

(28) The National Institute of Standards and Technology. http://webbook.nist.gov/chemistry. Accessed on 10/2009.

(29) Durig, D. T.; Esterle, J. S.; Dickson, T. J.; Durig, J. R. An Investigation of the chemical variability of woody peat by FTIR spectroscopy. *Appl. Spectrosc.* **1988**, *42*, 1239–1244.

(30) Genestar, C.; Palou, J. SEM Ű FTIR spectroscopic evaluation of deterioration in an historic coffered ceiling. *Anal. Bioanal. Chem.* **2006**, *384*, 987–993.

(31) Paatero, P.; Tapper, U. Positive Matrix Factorization Ű A Nonnegative Factor Model With Optimal Utilization Of Error-Estimates Of Data Values. *Environmetrics* **1994**, *5*, 111–126.

(32) Sive, B. C.; Zhou, Y.; Troop, D.; Wang, Y. L.; Little, W. C.; Wingenter, O. W.; Russo, R. S.; Varner, R. K.; Talbot, R. Development of a cryogen-free concentration system for measurements of volatile organic compounds. *Anal. Chem.* **2005**, *77*, 6989–6998.

(33) Zhou, Y.; Varner, R. K.; Russo, R. S.; Wingenter, O. W.; Haase, K. B.; Talbot, R.; Sive, B. C. Coastal water source of short-lived halocarbons in New England. *J. Geophys. Res.* **2005**, *110*, D21302.

(34) Holzinger, R.; Millet, D. B.; Williams, B.; Lee, A.; Kreisberg, N.; Hering, S. V.; Jimenez, J.; Allan, J. D.; Worsnop, D. R.; Goldstein, A. H. Emission, oxidation, and secondary organic aerosol formation of volatile organic compounds as observed at Chebogue Point, Nova Scotia. *J. Geophys. Res.* **2007**, *112*, D10S24.

(35) Sive, B. C.; Varner, R. K.; Mao, H.; Blake, D. R.; Wingenter, O. W.; Talbot, R. A Large Terrestrial Source of Methyl Iodide. *Geophys. Res. Lett.* **2007**, *34*, L17808.

(36) Zhou, Y.; Mao, H.; Russo, R. S.; Blake, D. R.; Wingenter, O. W.; Haase, K. B.; Ambrose; Varner, R. K.; Talbot, R.; Sive, B. C. Bromoform and dibromomethane measurements in the seacoast region of New Hampshire, 2002−2004. *J. Geophys. Res.* **2008**, *113*, D08305.

(37) Cliff, S. U.C. Davis 8-Stage Rotating DRUM Impactor Sampler Elemental Data. ftp://ftp.al.noaa.gov/UCD_Elemental_Data. Accessed on 01/2010.

(38) Pekney, N. J.; Davidson, C. I.; Zhou, L. M.; Hopke, P. K. Application of PSCF and CPF to PMF-modeled sources of $PM_{2.5}$ in Pittsburgh. *Aerosol Sci. Technol.* **2006**, *40*, 952–961.

(39) HYSPLIT−Hybrid Single Particle Lagrangian Integrated Trajectory Model. http://www.arl.noaa.gov/HYSPLIT.php. Accessed on 11/2009.
(40) Lee, E.; Chan, C. K.; Paatero, P. Application of positive matrix factorization in source apportionment of particulate pollutants in Hong Kong. *Atmos. Environ.* **1999**, *33*, 3201–3212.
(41) Andreae, M. O.; Atlas, E.; Harris, G. W.; Helas, G.; deKock, A.; Koppman, R.; Maenhaut, W.; Mano, S.; Pollock, W. H.; Rudolph, J.; Scharffe, D.; Schebeske, G.; Welling, M. Methyl halide emissions from savanna fires in southern Africa. *J. Geophys. Res.−Atmos.* **1996**, *101*, 23603–23613.
(42) Yokelson, R. J.; Susott, R.; Ward, D. E.; Reardon, J.; Griffith, D. Emissions from smoldering combustion of biomass measured by open-path Fourier transform infrared spectroscopy. *J. Geophys. Res.−Atmos.* **1997**, *102*, 18865–18877.
(43) Muhle, J.; Lueker, T. J.; Su, Y.; Miller, B. R.; Prather, K. A.; Weiss, R. F. Trace gas and particle emissions from the 2003 Southern California wildfires. *J. Geophys. Res.−Atmos.* **2007**, *112*, 1–12.
(44) Rasmussen, R. A.; Rasmussen, L. E.; Khalil, M. A. K.; Dalluge, R. W. Concentration distribution of Methyl Chloride in the atmosphere. *J. Geophys. Res.* **1980**, *85*, 7350–7356.
(45) Ayers, G. P.; Gillett, R. W.; Granek, H.; De Serves, C.; Cox, R. A. Formaldehyde production in clean marine air. *Geophys. Res. Lett.* **1997**, *21*, 401–404.
(46) Clarke, A. D.; Owens, S. R.; Zhou, J. C. An ultrafine sea-salt flux from breaking waves: Implications for cloud condensation nuclei in the remote marine atmosphere. *J. Geophys. Res.* **2006**, *111*, D06202.
(47) Louchouarn, P.; Opsahl, S.; Benner, R. Isolation and quantification of dissolved lignin from natural waters using solid-phase extraction and GC/MS. *Anal. Chem.* **2000**, *72*, 2780–2787.
(48) Hedges, J. I.; Keil, R. G.; Benner, R. What happens to terrestrial organic matter in the ocean. *Org. Chem.* **1997**, *27*, 195–212.
(49) Hernes, P. J.; Benner, R. Terrigenous organic matter sources and reactivity in the North Atlantic Ocean and a comparison to the Arctic and Pacific oceans. *Mar. Chem.* **2006**, *100*, 66–79.
(50) van Alstyne, K. L.; Paul, V. J. The biogeography of polyphenolic compounds in marine macroalgae: temperate brown algal defenses deter feeding by tropical herbivorous fishes. *Oecologia* **1990**, *84*, 158−164.
(51) Abdala-Diaz, R. T.; Cabello-Pasini, A.; Perez-Rodriguez, E.; Conde Alvarez, R. M.; Figueroa, F. L. Daily and seasonal variations of optimum quantum yield and phenolic compounds in Cystoseira tamariscifolia (Phaeophyta). *Mar. Biol.* **2006**, *145*, 459–465.
(52) Manley, S. L.; Dastoor, M. N. Methyl Halide production from the gianty-kelp, macrocystis, and estimated of global CH_3I production by kelp. *Limnol. Oceonogr.* **1987**, *32*, 709–715.
(53) Moore, R. M. Methyl halide production and loss rates in sea water from field incubation experiments. *Mar. Chem.* **2006**, *101*, 214–219.
(54) Kettle, A. J.; Rhee, T. S.; von Hobe, M.; Poulton, A.; Aiken, J.; Andreae, M. O. Assessing the flux of different volatile sulfur gases from ocean to atmosphere. *J. Geophys. Res.−Atmos.* **2001**, *106*, 12193–12209.
(55) Hawkins, L. N.; Russell, L. M.; Covert, D. S.; Quinn, P. K.; Bates, T. S. Carboxylic Acids, Sulfates, and Organosulfates in Processed Continental Organic Aerosol over the Southeast Pacific Ocean during VOCALS-REx 2008. *J. Geophys. Res.* **2010**, in press. Doi: 10.1029/2009JD013276.
(56) Jordan, C.; Fitz, E.; Hagan, T.; Sive, B. C.; Frinak, E.; Haase, K.; Cottrell, L.; Buckley, S.; Talbot, R. Long-term study of VOCs measured with PTR-MS at a rural site in New Hampshire with urban influences. *Atmos. Chem. Phys.* **2009**, *9*, 4677–4697.

ES9032277